

Synthesis, characterizations, and comparative study of electro-optical properties of indole-based squaraine sensitizers as efficiency to enhancing dye-sensitized solar cells

Sultan A. Al-horaibi, S.T. Gaikwad, Anjali S. Rajbhoj*

Department of Chemistry, Dr. Babasaheb Ambedkar Marathwada University, Aurangabad, Maharashtra 431001, India

*Corresponding author

DOI: 10.5185/amlett.2018.1457

www.vbripress.com/aml

Abstract

Squaraine dyes (*SQ*) have acquired sufficiently great attention as dye-sensitized solar cell (DSSCs) materials. In the present study, we have synthesized and characterized of two novel symmetrical sensitizers dyes for dye-sensitized solar cells which contain electron withdrawing ($-\text{COOH}$) group with long alkyl ester chain (*SQ1*) and another without encoring group (*SQ2*). We have investigated the structural, electronic, photo-electrochemical, and charge transport properties of two *SQ1* & *SQ2* indole-based squaraine dyes. The ground state geometry has been computed by applying density functional theory (DFT). The excitation energy and the oscillator strength were calculated by using time-dependent (DFT-TD) at DFT/B3LYP/6-31G** level of theory. We have focused and study on the frontier molecular orbitals (HOMO and LUMO), electron injection (ΔG^{inject}), light harvesting efficiency (*LHE*), open-circuit voltage (V_{oc}), relative electron injection (ΔG^{inject}), and short-circuit current density (J_{sc}). The effect of $-\text{COOH}$ as (acceptor) and $-\text{OCH}_3$ (donor) groups on *SQ1* and *SQ2* were investigated. The factors affecting, ΔG^{inject} , *LHE*, V_{oc} and J_{sc} revealed that *SQ1* would be more favourable to enhance the performance of DSSCs. The theoretical calculations and absorbance results show that the electron density of LUMO of *SQ1* is delocalized in the whole chromophore, leading to strong electronic coupling between *SQ1* and TiO_2 surface. So, the *SQ1* sensitized solar cells exhibit better photovoltaic performance. Copyright © 2018 VBRI Press.

Keywords: Dye-sensitized solar cell, squaraine dyes, computational analyses, DFT-TD.

Introduction

Dye sensitized solar cell is one of the best promising alternative renewable energy sources. The dye sensitized solar cell (DSSCs) is a nanostructured photo-electrochemical device. Light is absorbed by a dye attached to the surface of a mesoporous wide band gap semiconductor. Solar energy is transformed into electricity via the photo-induced injection of an electron from the excited dye into the conduction band of the semiconductor. The electrons move through the semiconductor to a current collector and external circuit. A redox mediator in the pores ensures that oxidized dyes are continuously regenerated and this process is cyclic [1]. New ways of manufacturing solar cells that can scale up to large volumes and at low cost are required. DSSCs considered a technology between the second and third-generation solar cells reported in 1991 by O'Regan, and Grätzel [2]. DSSCs are built of a dye absorbed wide band gap semiconductor electrode (TiO_2 or ZnO), an electrolyte containing the I^-/I_3^- redox couple, and a Pt-coated counter electrode [3–10], (Fig.1). The electron injection into the semiconductors and dye regeneration

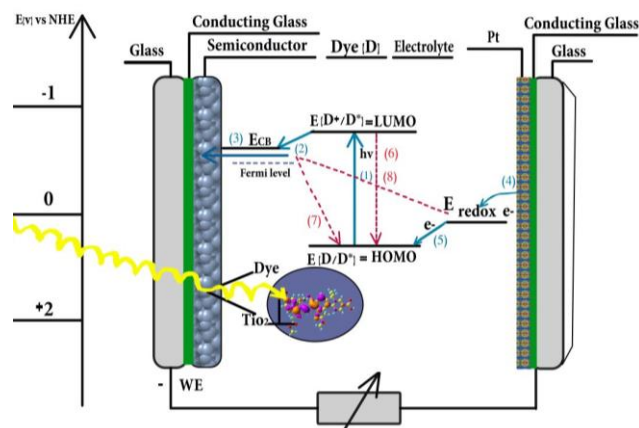


Fig. 1. The processes in operational DSSCs. Blue arrows indicate beneficial processes and red arrows indicate undesired losses.

with hole transfer to the redox electrolyte, called sensitizer in DSCs which is one of the most critical component to for the light harvesting and the charge separation process [11]. Recently, Gratzel et al. reported using a co-sensitizer in DSSC, i.e. a zinc porphyrin dye

(YD 2-o-C8) and an organic dye (Y123) in conjunction with a tris (2, 2' bipyridine) cobalt (II/III) I/I_3^- redox couple, this provided DSSCs to reach 12.3% efficiency [12]. In the near-infrared (NIR) region the photoelectric conversion efficiency of DSSCs is insufficient, so further studies are needed to develop new sensitizers to enhanced light-harvesting in whole range of the spectra of sunlight, including visible and NIR regions light [13]. Squaraine (SQ) dyes are considered one of the best substitutes between the different Ru-free organic dyes available. They have higher molar extinction coefficients and much cheaper Ru-free organic dyes (e.g. extension coefficient of squaraine is $\sim 3 \times 10^5 \text{ M}^{-1}\text{cm}^{-1}$) [14-16], than conventional dyes (Ru complexes is $\sim 1 \times 10^4 \text{ M}^{-1}\text{cm}^{-1}$) [17]. They have ability to absorb photons with a long wavelength in the range, 500 ~700 nm. In addition, SQ dyes are used to aggregate very easily on the TiO_2 surface, which reduce the solar cell performance [18, 19] and their absorption band is very narrow compared to Ru-complexes [14-16]. It will be huge challenge to develop novel SQ dyes in enhancing and production of high efficiency DSSCs. In previous studies, the electronic/charge transport properties and efficiency of DSSCs have been developed by incorporating thiophene, pyrrole, thiazole, and indole unit(s) into squaraine dyes [20-22]. Bridge elongation, introduction of electron-withdrawing groups and/or push-pull strategies are good approaches to enhance the efficiency, intra-molecular charge transfer (ICT) and stability of sensitizers. Larger light harvesting ability [23-27]. ICT and electronic coupling constants [light harvesting efficiencies (LHE)] would lead to more efficient DSSCs. Dye aggregation and charge recombination generally leads to lower efficiency [28-33]. In the present paper, we have synthesized of two novel squaraine sensitizers *SQ1* & *SQ2* and compared them. The novel carboxylic indole squaraine sensitizer and another without carboxylic group were synthesized calculated by Gaussian03 package (Fig.4). The *SQ1* containing double-carboxylic acid acceptor/anchor was more efficient between the photo sensitizing dye and TiO_2 , forming stronger electronic coupling and the more strongly accepting attached carboxylic acid with TiO_2 . The ethoxy groups and an alkyl chain at the N-atom of indole decreases the aggregation of dyes and charge recombination. These two types of squaraine sensitizers exhibited a panchromatic response from the visible region to the NIR region. All two (*SQ1* and *SQ2*) squaraine sensitizers have long side chains and acidic ligands which lead to inhibit recombination and decreased aggregation as a result to rotation of the molecule freedom without hinder, resulting in improved dye-sensitized solar cell efficiency. The investigation was accomplished through shedding some light on the dye/ electro-optical properties, electron injection (ΔG^{inject}) and light harvesting energy (LHE). Also, in this paper, we have discussed the characterizations of two symmetric squaraine dyes with alky ester chain donating groups which supply strong electronic coupling to CB of the TiO_2 . In addition, the optoelectro-chemical properties of the two indole-based dyes were investigated. Finally, the factors affecting of

short-circuit current density (J_{sc}) and open-circuit voltage (V_{oc}), were studied and concluded with a discussion on the nature of sensitizers, based on the previously mentioned information [29,50]. The *SQ1* was observed to be red-shifted i.e. to a longer wavelength than the other sensitizer because of the di-carboxyl groups. The absorption spectrum of *SQ1* was red-shifted more than that of *SQ2* due to two-electrons accepting of di-carboxylic acid. This is lead to the extension of the optical absorption wavelength region improved light harvesting and enhanced the molar extinction coefficients.

Experimental

Materials

All chemicals, 4-Hydrazinobenzoic acid (HBA, 98%) Phenyl hydrazine (97%), Squaric acid (98%), Sodium Acetate Anhydrous (>99%), Sodium carbonate anhydrous (Na_2CO_3 , powder, 99.999% trace metals basis) from Sigma-Aldrich. Isopropyl methyl ketone (3-Methyl-2-butanone, 98%), Sodium sulphate anhydrous (Na_2SO_4 99%), Methyl 3-bromopropionate (97%), Ethyl acetate (EtOAc, 99%), Toluene (99%) from (Alfa Aesar), n-Butanol (SISCO research laboratories PVT-LTD), Diethyl ether (Et_2O , 98%, Molychem), Acetonitrile (98%, Molychem) Alfa Aesar, Methanol (MeOH, 99.8%, Sigma-Aldrich), Squaric acid (98+%), Methanol (MeOH, 99%, Alfa Aesar), Ethanol (EtOH, 98%, Sigma-Aldrich), petroleum ether 60/80 (Alfa Aesar), Silica gel, 60-120 mesh, for column chromatography (Vetec), (Sigma-Aldrich).

Characterizations

NMR spectra were recorded on Bruker AVANCE III WM 600 and 400 spectrometers (Karlsruhe, Germ -any) and ^{13}C MHz NMR at 150MHz. Tetramethylsilane (TMS) was used as internal standard. The chemical shifts were recorded in parts per million (ppm) with TMS as the internal reference. FTIR spectra of samples (as KBr pellets) were obtained using a Nicolet 6700 Thermo Scientific instrument equipped with a diamond ATR probe, over the range 400–4000 cm^{-1} . UV-vis spectra were obtained using a PerKin Elmer Lambda 950 spectrophotometer. Melting points (M.p) were measured with a melting point apparatus "Dr. Tottoli" from Büchi. They were determined in open capillary tubes. Optimized geometries of final dye with the highest occupied molecular orbital (HOMO) and lowest unoccupied molecular orbital (LUMO) were calculated at B3LYP/6-311G** level of calculations using Gaussian 03 program package.

Synthesis of 2, 3, 3-trimethyl-3H-indole-5-carboxylic acid (1)

A round bottom flask (250 ml) fitted with condenser, containing a mixture of 4-hydrazinylbenzoic acid (10g, 65.7 mmol) and 3-methyl butan-2-one (8.90g, 103 mmol) with sodium acetate anhydrous (11g, 134mmol) in glacial acetic acid (160 ml) were stirred for 1h at room temperature. After that it was refluxed for 9h and then it

was cooled to room temperature. The solvent was removed by distillation under reduced pressure. 10% MeOH (1:9 MeOH /H₂O v/v) was added to the output to give precipitate which was filtered and washed with water. Recrystallization with ethyl acetate gave, 2, 3, 3-trimethyl-3H-indole-5-carboxylic acid (1) as orange powder in 60.4 % yield, m.p = 205-210 °C. ¹HNMR (400MHz-CDCl₃) spectrum recorded at δ (ppm) 1.25 (s, 6H,2CH₃), 2.25 (s,3H,CH₃), 7.5(d,1H, J=7.8 Hz, Ar-H), 7.90 (d, 1H, J=8.9Hz,Ar-H), 7.99(s,1H,Ar-H).¹³C-NMR(400 MHz -CDCl₃)16.9,25.44.25,44.25, 42.4, 122.8,127.4, 127.8 127.9, 146.6, 148.2, 164.9, 169.1.

Synthesis of 2, 3, 3-trimethyl-3H-indole (2)

In a round bottom flask phenyl hydrazine (5.40 g, 50 mmol) and isopropyl methyl ketone were added dropwise (4.40 g, 50 mmol), then the solution was heated with stirring at 85°C for 24h, an then cooled to room temperature . 40 ml of H₂O was added and extracted by Et₂O (3*30 ml), after that dried over Na₂SO₄ for 30 minutes, filtered and washed by Et₂O to get a crude red liquid (98%). The obtained liquid was dissolved in acetic acid (18 ml) and then the mixture was heated with stirring at 90 °C for 1.5 h and then cooled to room temperature. The mixture was neutralized with saturated Na₂CO₃ and extracted by ethyl acetate (3*25 ml), dried over Na₂SO₄ for 30 minutes. It was then filtered and washed by ethyl acetate, the liquid residue was collected to give the yellow oil product in yield= 85%. ¹HNMR (400MHz-CDCl₃) spectrum recorded at δ(ppm) 1.27 (s, 6H, 2CH₃), 2.22(s,3H,CH₃), 7.16 (t,1H, J = 0.88 Hz, Ar-H), 7.27(d,t, 2H, J= 1.24 Hz, Ar-H), 7.53(d, 1H, J= 7.6 Ar-H).¹³C-NMR (400MHz -CDCl₃), 15.25(CH₃), 22.94 (2CH₃), 53.45(C₃), 119. 70, 121.19, 125, 127. 46 (Carbon phenyl aromatic), 145.47, 153.41 (C₇, C₈ respectively), 187.95 (C₂).

Synthesis of 5-carboxy-1-(3-methoxy-3-oxopropyl)-2, 3, 3-trimethyl-3H-indolium bromide (3)

A mixture of compound 2, 3, 3-trimethyl-3H-indole-5-carboxylic acid (1), (2g, 12.5 mmol) and methyl 3-bromopropanoate (5.25g, 31.43 mmol) in 10 ml acetonitrile were refluxed under N₂ atmosphere for 24 h. It was then cooled. The solvent was removed by distillation under reduced pressure. Diethyl ether was added to the output several times to remove starting material. It was then recrystallized from ethyl acetate and 2 drops ethanol to give pink coloured compound (3) as a Yield = 49%. ¹HNMR (400 MHz-CDCl₃) spectrum recorded at δ(ppm) 1.63(s,6H,2CH₃), 2.25 (s, 3H, CH₃), 3.23(t, 2H, J= 6Hz, CH₂-CO-), 3. 63(s, 3H, J= 6.5Hz, CH₃-O), 5.14 (t, 3H, J = 6.67 Hz, CH₂-N⁺), 7.5(d, 1H, J=7.8Hz, Ar-H), 7.90 (d, 1H, J = 8.9Hz, Ar -H), 7.99(s, 1H, Ar-H). ¹³C-NMR (400 MHz-CDCl₃) spectrum recorded at 9.33 (CH₃), 25.44 (2CH₃), 29.1 (C₃), 29. (-CH₂ -CO), 42.4(-CH₂-N⁺), 50.29(CH₃-CO), 122.79, 124.6, 127.79, 130.6, 146.6, 148.2(Carbon phenyl), 169.1(-COOH), 171.9(-C=O), and 191.5(-C=N).

Synthesis of 1-(3-methoxy-3-oxopropyl)-2, 3, 3-trimethyl-3H-indolium bromide (4)

In a round bottom flask 2, 3, 3-trimethyl-3H-indole (2.65 g, 16.4 mmol) and methyl 3-bromopropanoate (6.45g, 41.25 mmol) were taken and then the mixture was refluxed under N₂ atmosphere for 23 h. cooled to room temperature, then Et₂O was added and filtered off to give pink solid produced from 1-(3-methoxy-3-oxopropyl) -2,3,3-trimethyl-3H-indolium bromide, (4.95g, yield = 85%). The product was recrystallized from ethyl acetate and 2drops from methanol, m.p =145-150 °C. The IR spectrum showed absorption bands at γ (cm⁻¹): 3433 (broad OH), 3004 (stretch C-H), 2839 (stretch C-H), 1730 (stretch C=O), 1674 (C=C), 1589 (C=N), 1461(bending CH₂), 1355(bending CH₃), 1264 (C-O), 1222(C-N). ¹HNMR (400 MHz-CDCl₃) spectrum was recorded at δ1.63 (s, 6H, 2CH₃), 3.17(s, 3H, CH₃), 3.23(t, 2H, J= 6Hz, CH₂-CO-), 3.63(s, 3H, CH₃ -O-CO), 5.14(t, 3H, J=6Hz, CH₂-N-Ar), 7.5-7.60 (m, 1H, Ar-H), 7.92(d, 1H, J=3.6Hz, Ar -H). ¹³C-NMR (400 MHz-CDCl₃) spectrum recorded at 16.62(CH₃), 23 (2CH₃), 31.1 (CH₂-CO), 45.6(C₃), 52.3(CH₂-N), 54.7 (CH₃-O), 115.9-141.4 (phenyl carbons), 170.8 (C=O), 198.31 (C=N).

Synthesis of squaraine dye (SQ1)

A mixture of 5-carboxy-1-(3-methoxy-3-oxopropyl)-2,3,3-trimethyl-3H-indolium bromide (1g, 3.16 mmol) and 3,4-dihydroxycyclobut-3-ene-1, 2-dione (0.18g ,1.58 mmol) was taken in mixture of n-butanol / toluene (60 mL, 1:1v/v). Reaction mixture was refluxed for 24h using Dean-Stark trap for azeotropic removal of water. After completion of reaction, the reaction mixture was cooled and the solvent was evaporated. Filtered and washed with chloroform. The product was purified by silica gel column chromatography with chloroform and methanol (10: 0.5 v/v), recrystallized by ethyl acetate and petroleum ether to give **SQ1** (see **scheme 1.**), dark-blue solid with 51.72 % yield. ¹HNMR (400 MHz-CDCl₃) spectrum recorded at δ(ppm) 1.63 (s,6H,2CH₃), 1.83 (s, 6H, 2CH₃), 2.5(t,2H,-CH₂-CO-), 2.8(t, 2H,-CH₂-CO-), 3.61(s,6H, 2CH₃-O), 3.79(t,2H,-CH₂-N), 4.12 (t,2H,-CH₂-N⁺), 5.99(s, 1H, -CH=C-), 6.62(s,1H,-CH =C-), 7.33(d,1H,J= 8.4Hz, Ar-H), 7.58(s,1H, Ar-H), 7.62 (d, 1H,J = 7.33Hz, Ar-H), 7.79(d,1H,J = 8.4 Hz, Ar-H), 7.90(d,1H,J=1.78Hz, Ar-H), 8.22(s,1H, Ar-H). ¹³C-NMR (400MHz-CDCl₃) 25.42, 29.4, 31.51, 32, 42, 42. 35, 43.5, 49.56, 51.76, 53.75, 106.11, 117 .23, 119.10, 122.66, 124.54, 127.65, 129.18, 130.63, 133.37, 137. 42, 143.23, 149.5, 168.2, 171.5, 171.8, 173.3, 194.5.

Synthesis of squaraine dye (SQ2)

A mixture of 1-(3-methoxy-3-oxopropyl)-2, 3, 3-trimethyl-3H-indolium bromide (1g, 3.17 mmol) and 3, 4-dihydroxycyclobut-3-ene-1,2-dione (0.297g, 1.59 mmol) was taken in n-butanol/ toluene (50 mL, 1:1v/v). Reaction mixture was refluxed for 24 h using Dean-Stark trap for azeotropic removal of water. After completion of reaction, the reaction mixture was cooled and the solvent

was evaporated. The product was purified by silica gel column chromatography with chloroform and methanol (10:1 v/v), recrystallized by ethyl acetate and petroleum ether to give **SQ2** (see **scheme 1**.) dark-blue solid in 61.87% yield. ¹H-NMR (400MHz-CDCl₃) spectrum recorded at δ 1.3(s,6H,2CH₃), 1.55(s, 6H, 2CH₃), 1.8(t,2H,N⁺-CH₂), 2.3 (t,2H,-CH₂-CO), 2.5(t, 2H,CH₂-CO-), 3.8 (s,6H, 2CH₃-O), 5.9(s,1H,C=CH-aliphatic), 7.10 (d, 2H, J=7.8Hz, Ar-H), 7.15(t, 2H, J=0.6Hz,Ar-H), 7.26 (s,1H,C=CH- aliphatic), 7.32(t, 2H, J=0.6 Hz, Ar-H), 7.36(d, 2H, J=7.2Hz, Ar-H). ¹³C-NMR (400MHz-CDCl₃) 25.42, 29.4, 31.51, 32.42, 42.35, 43.5, 49.56, 51.76, 53.75, 106.11, 116.3 117.23, 119.10, 122.66, 124.54, 127.65, 129.18, 130.63, 133.37, 137.42, 143. 23, 149.5, 168.2, 173.3.

Computational analyses of squaraine sanitizers (SQ1 & SQ2)

The theoretical calculations carried on in the present work by applied results of density functional theory (DFT) and time-dependent (TD-DFT). Density functional theory is good approach that reproduces experimental evidence for small organic molecules, among different functional, B3LYP provides the best depiction [39-46]. The charge transport properties and experimental electronic have been generated by applying the B3LYP/6-31G** level of theory [41]. Electro injection was applied by Preet and co-workers [30,47] for some organic compounds and furnished that the B3LYP/6-31G** level of theory is sufficient. In the present study, electronic properties and ground state geometries were computed at DFT/B3LYP/6-31G**. By applying polarizable continuum model (PCM) excitation energies were calculated. the free energy change for electron injection onto TiO₂ surface and excited state oxidation potential of the dye were calculated using mathematical equations.

The calculation of free energy change for electron injection has been used this equation [13]:

$$\Delta G^{inject} = E_{ox}^{dye*} - E_{CB}^{TiO_2} \quad (1)$$

where E_{ox}^{dye*} is the oxidation potential of the dye in the excited state. $E_{CB}^{TiO_2}$ is the energy of conduction band on titanium dioxide (TiO₂). Because of highly sensitive $E_{CB}^{TiO_2}$ to the conditions, accurate determination of the conduction band edge of TiO₂ is very difficult, so we used experimental value to $E_{CB}^{TiO_2} = -4.0$ eV [13,48-49].

E_{ox}^{dye*} was calculated using following equation:

$$E_{ox}^{dye*} = E_{ox}^{dye} - \lambda_{max}^{ICT} \quad (2)$$

where λ_{max}^{ICT} is the energy of intermolecular charge transfer (ICT), the light harvesting efficiency (LHE) is determined by the following formula:

$$LHE = 1 - 10^{-A} = 1 - 10^{-f} \quad (3)$$

where $A(f)$ is the oscillator strength of the dye associated with λ_{max}^{ICT} which is found directly from TD-DFT calculation as follow:

$$f = \frac{3}{2} \lambda_{max}^{ICT} \left| \mu_o - \mu_{ICT} \right|^2 \quad (4)$$

where μ_{ICT} is the dipolar transition moment associated to the electronic excitation, the efficiency (η) of dye sensitized solar cell was determined using the following formula:

$$\eta = FF = \frac{V_{oc} J_{sc}}{P_{inc}} \quad (5)$$

where J_{sc} is the short-circuit current density, V_{oc} the open-circuit voltage, FF the fill factor, and P_{inc} the intensity of the incident light. The J_{sc} was determined using the following equation:

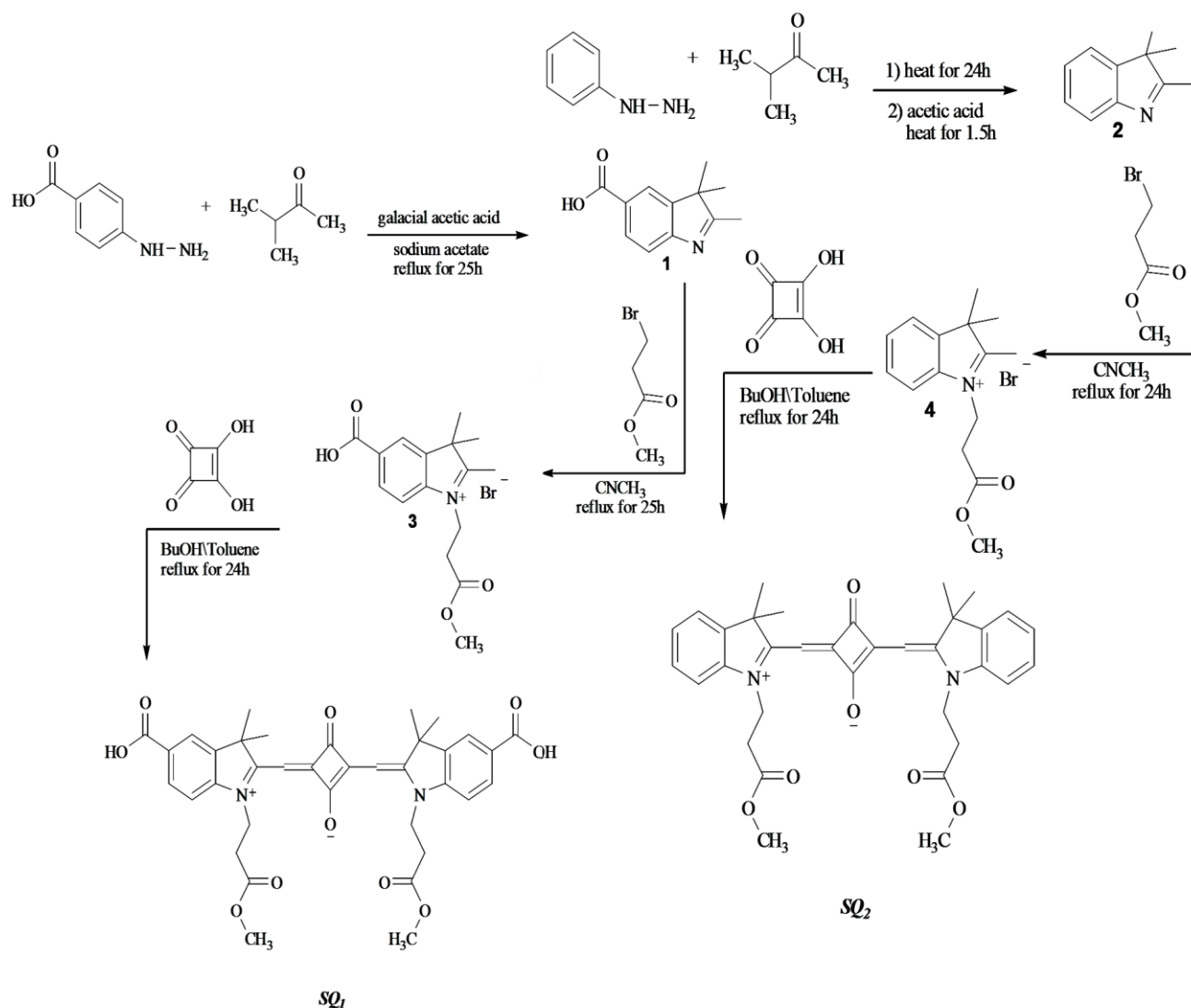
$$J_{sc} = \int_{\lambda} LHE(\lambda) \phi_{inject} n_{collection} d\lambda \quad (6)$$

where $n_{collection}$ is the charge collection efficiency, which is constant. From Eq.6, we can find that J_{sc} is linked directly with the LHE . The ϕ_{inject} is electron injection efficiency related to ΔG^{inject} . The higher LHE and ΔG^{inject} would lead to efficient dye sensitized solar cells [50].

Result and discussion

Synthesis of squaraine dyes

Symmetrical dicarboxylic-substituted squaraine dyes **SQ1** were synthesized in three steps from 4-hydrazinyl benzoic acid as shown in **Scheme 1**. The synthetic route includes the reaction of 4-hydrazinylbenzoic acid (1 equivalent), with 3-methyl butan-2-one (1.5 equivalent) to afford the 2, 3, 3-trimethyl-3H-indole-5-carboxylic acid (**1**) in 60.4% yield, which was subsequently converted to heterocyclic quaternary salt with 2.5 equivalent from methyl 3-bromopropanoate in the presence of acetonitrile to give **3** in 49 % yield. The subsequent condensation of 2 equivalent of indolium salt **3** and 1 equivalent of squaric acid under reflux in butanol /toluene mixture to afford the symmetrical squaraine dye **SQ1** in 51.72% yield. The synthesis of symmetrical squaraine dyes **SQ2** was performed as depicted in **Scheme 1**. In the first step, phenyl hydrazine was treated with 1 equivalent of isopropyl methyl ketone in the presence of Acetic acid to afford 2, 3, 3-trimethyl-3H-indole (**2**) in 85% yield. Subsequent quaternization of **2** using excess of methyl 3-bromopropanoate in the presence of acetonitrile led to 1-(3-methoxy-3-oxopropyl) -2, 3, 3-trimethyl-3 H-indolium bromide (**4**) in 85 % yield. Condensation of 2 equivalent of indolium salt **4** and 1 equivalent of squaric acid under reflux in butanol/toluene mixture to afford the symmetrical squaraine dye **SQ2** in 61.87 % yield (**Scheme.1**).



Scheme 1. Synthesis routes of squaraine sensitizers (SQ_1 & SQ_2) for dye-sensitized solar cells.

Photophysical characterization

In (Fig 2.), (a,b) shows the normalized UV-Vis absorption spectra; bands maxima of SQ_1 and SQ_2 dissolved in DCM are observed at 637 and 634 nm, respectively and their corresponding high molar extinction coefficient values 67543 and $64567 \text{ mol}^{-1}\text{Lcm}^{-1}$ are in agreement with $\pi-\pi^*$ transitions, could be observed in the SQ_1 and SQ_2 (see Fig 3.). The SQ_1 was observed to be red-shifted than the other sensitizer because of the di-carboxyl groups. The absorption spectrum of SQ_1 was red-shifted more than that of SQ_2 due to two-electrons accepting di-carboxylic acid. This leads to the extension of the optical absorption wavelength region, improved light harvesting and enhanced the molar extinction coefficients.

Geometries

We have presented geometrical parameters of two indole based squaraine dyes in Table 1. The C_3-C_4 , C_7-O_2 and C_8-O_1 bond lengths shortened while C_1-C_2 , C_2-C_3 and

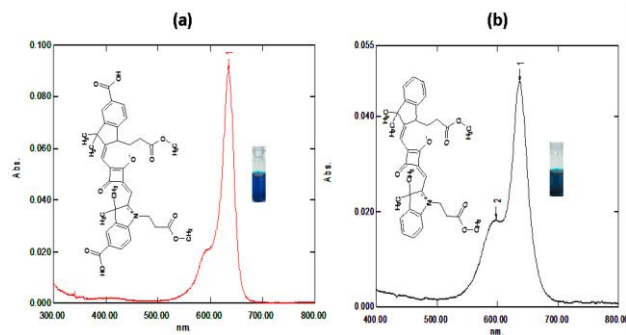


Fig 2. (a,b). The UV absorption spectra of SQ_1 (a) and SQ_2 (b) sensitizers at a concentration of $1 \times 10^{-5} \text{ M}$ in DCM.

C_1-N_1 lengthened compared to SQ_2 . The C_1-C_2 , C_2-C_3 and C_4-N_1 bond lengths shortened while C_1-N_1 , C_3-C_4 , C_7-O_2 , C_8-O_1 lengthened compared to SQ_1 . The $C_1-N_1-C_4$, $C_4-C_5-C_6$, $C_6-C_8-O_1$ bonds angles shortened while $C_2-C_3-C_4$, $C_6-C_7-O_2$ lengthened compared to SQ_1 . When $-\text{COOH}$ group

is substituted at $-R$ position then C_1-N_1 , C_3-C_4 usually shortened while C_4-N_1 , C_2-C_3 bond distances lengthened than $SQ2$. It is might be due to the moderate electron withdrawing groups which are in the same side which influence geometry more than isomers without carboxylic groups. Thus, in form geometric variation in $SQ1$ is smaller than the $SQ2$. The electron charge density pull /donating by electron pull /electron donating groups results in shortening / lengthening of bond-lengths while are in good agreement with previous studies [51].

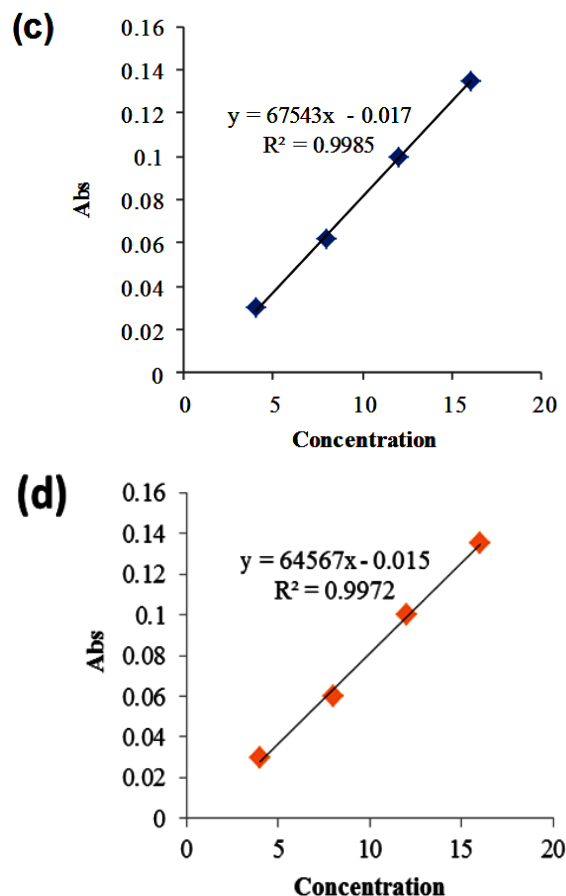


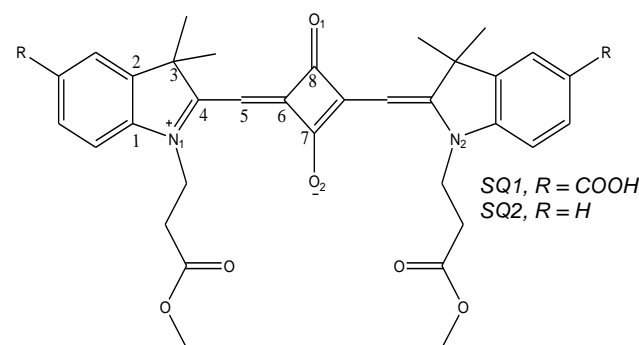
Fig 3. (c,d). The extinction coefficients of $SQ1(c)$ and $SQ2(d)$ sensitizers at a concentration of 1×10^{-3} M in DCM solution with different concentrations, 2×10^{-4} , 4×10^{-4} , 6×10^{-4} , 8×10^{-4} M at 637 and 634 nm, respectively.

Frontier molecular orbitals and absorption spectra

In the charge density distribution patterns of the ground state highest occupied molecular orbitals (HOMOs and HOMOs-1), lowest unoccupied molecular orbitals (LUMOs and LUMOs+1) of two $SQ1$ and $SQ2$ indole-based squaraine dyes are illustrated in **Fig 4**. The HOMOs-1 is distributed on squaraine moiety and only on right indole moiety in $SQ1$ while distributed on the squaraine moiety and both of the indole units in $SQ2$. The charge densities of LUMO and HOMO are localized on squaraine moieties. In $SQ1$, the electron-withdrawing group is $-COOH$ and the carbonyl groups of 2-3-(2-

methoxy-2-oxomethyl) units also take part in the formation of LUMOs and LUMOs+1 in $SQ1$ and $SQ2$. The LUMOs+1 are localized on both of the left indole units and squaraine moieties. The charge density on carbonyl LUMO and LUMO+1 on 2-3-(2-methoxy-2-oxomethyl) are less than $SQ2$ -counterpart. The computed energies of HOMO (E_{HOMOs}), LUMO (E_{LUMOs}), and LUMOs+1 ($E_{LUMOs+1}$) and energy gaps (E_g) of two $SQ1$ and $SQ2$ indole-based squaraine dyes at B3LYP/6-31G** level of theory are illustrated in **Table 2**. The E_{HOMOs} , E_{LUMOs} and $E_{LUMOs+1}$ increases in $SQ2$ while $SQ1$ decreases substituting the electron withdrawing group $-COOH$.

Table 1. The geometrical parameters, bond lengths (Å) and bond angles (°) of indole-based $SQ1$ & $SQ2$ optimized at B3LYP/6-31G** level of theory.



	$SQ1$	$SQ2$		$SQ1$	$SQ2$
	Bond lengths			Bond angles	
C_1-C_2	1.398	1.403	$C_1-N_1-C_4$	1.399	1.404
C_1-N_1	1.415	1.403	$C_2-C_3-C_4$	1.415	1.403
C_2-C_3	1.517	1.522	$C_4-C_5-C_6$	1.378	1.390
C_3-C_4	1.545	1.536	$C_6-C_7-O_2$	1.546	1.537
C_4-N_1	1.378	1.390	$C_6-C_8-O_1$	1.517	1.522
C_7-O_2	1.248	1.247			
C_8-O_1	1.231	1.230			

We have observed the smallest E_g values for $SQ1$, which has $-COOH$ group at the $-R$ position. The calculated energy gaps (E_g) of all the two squaraine $SQ1$ & $SQ2$ sensitizers are smaller than that of the dyenitro (2.81eV) [27] revealing that the absorption spectra of formers would be red shifted and that DSSC efficiency might be improved in the sensitizers $SQ1$ and $SQ2$. The smaller E_{LUMO} of $SQ1$ reveals that the injected electrons would be more stable, and the charge transport cannot be quenched in prior ones. The $SQ1$ sensitizer has $-COOH$ group which is good light harvesting site as well as would be helpful to anchor with the TiO_2 surface. $SQ1$ also, enhances solubility in solution and diminishes aggregation on TiO_2 [52]. In (**Fig 4**), the charge density distribution on LUMOs, is expected on $SQ1$ to be more stable after anchoring with the TiO_2 surface. Furthermore, $-COOH$ would be a favorable site from which to transfer

electrons from dyes to the TiO₂ surface. Generally, the acidic ligand would lead to enhance the solubility in solution and reduce aggregation [53]. The long side chains in acidic ligands lead to produce a barrier between holes in the redox couple and electrons in the TiO₂ to hinder recombination. In previous study, they have shed light on the charge transport behavior with respect to the size of the TiO₂ and found that the ICT forms dye with TiO₂ crystal [54]. The inorganic materials, e.g., TiO₂, in the photovoltaic devices would overwhelm the photo-induced degradation of the dyes. Moreover, the photo-generation of charge transporters would lead to excitons being absorbed by the TiO₂ [55, 56]. Additionally, absorption yield can be enhanced by incorporating TiO₂ [57]. The computed oscillator strengths (*f*), absorption wavelengths (λ), and major transitions of Indole-based squaraine *SQ1* and *SQ2* at absorption wavelengths (λ_a) of indole-based *SQ1* and *SQ2* (in dichloromethane) at B3LYP/6-31G** and TD-B3LYP/6-31G** level of theories.

Table 2. The calculated highest occupied molecular orbital energies (E_{HOMO}), lowest occupied molecular orbital energies (E_{LUMO}), LUMO+1 energies (E_{LUMO+1}), energy gaps (E_g)

	$E_{HOMO}(eV)$	$E_{LUMO}(eV)$	$E_{LUMO+1}(eV)$	$E_g(eV)$	$\lambda_a(nm)^a$	f^b	Transition
^a Dytenitro	-6.43	-3.62	-	2.82	529	1.324	H->L
<i>SQ1</i>	-4.98	-2.76	-1.33	2.25	625	1.980	H->L
<i>SQ2</i>	-4.69	-2.43	-0.44	2.31	619	1.719	H->L

^aExperimental λ_a in DCM = 637, 634 nm

Detail can be found in reference [29, 60], ^bOscillator strength

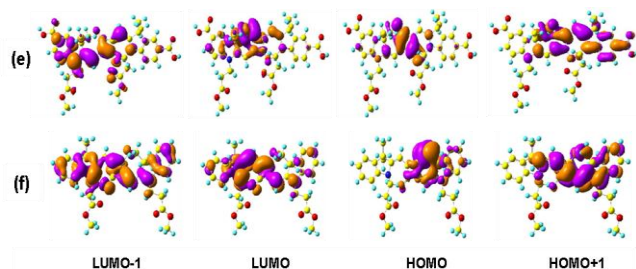


Fig. 4. The charge density distribution of the frontier molecular orbitals (0.02 contour value) of indole-based *SQ1* (e) & *SQ2* (f) at B3LYP/6-31G** level of theory.

Table 3. The comparative study of ΔG^{inject} , ΔG_r^{inject} , oxidation potential, light harvesting efficiency (LHE) of previously reported with present investigated *SQ1* and *SQ2* dyes in DCM at TD-B3LYP/6-31G** level of theory.

Compound	ΔG^{inject} (eV)	E_{ox}^{dye} (eV)	E_{ox}^{dye*} (eV)	λ_{max}^{ICT} (eV)	<i>f</i>	LHE	ΔG_r^{inject} (eV) ^a	References
^b Dytenitro	-0.39	5.96	3.61	2.35	1.319	0.9520	1.00	[29]
<i>SQ1</i>	-0.98	5.19	3.14	1.98	1.919	0.9985	2.75	[50,60]
<i>SQ2</i>	-1.40	4.91	2.86	2.05	1.804	0.9848	3.45	
Cis- <i>SQ1</i>	-0.96	5.05	3.04	2.01	1.890	0.9871	2.45	[50,58,60]
Cis- <i>SQ2</i>	-1.24	4.83	2.76	2.07	1.714	0.9807	3.18	

^aDetail can be found in reference [29,50, 60], ^b ΔG_r^{inject} = relative electron injection ΔG^{inject} (dye) / ΔG^{inject} (Dytenitro)

Short-circuit current density (J_{sc})

The comparative study of some previously reported dyenitro, Cis-SQ dyes and present work for *SQ1* & *SQ2*. The ΔG^{inject} , LHE, and ΔG_r^{inject} of indole-based squaraine sensitizers for DSSc are showed in **Table 3**. The negative calculated values of ΔG^{inject} showed that the excited state of the dye lies above the conduction band edge (CB) of TiO₂ resulting good condition for electron injection, it can be seen from Eq. 6, that the improvement of the short-circuit current density (J_{sc}), i.e., LHE and Φ_{inject} are two major factors which influence and enhance the J_{sc} . The electron injection efficiency (Φ_{inject}) is related directly to the light-harvesting efficiency (LHE).

TD-B3LYP/6-31G** level of theory is in good agreement with the experimentally measured values of 637, 634 nm respectively (see **Table 2**). The major transitions have been observed from H->L in two indole-based *SQ1* and *SQ2* sensitizers. The computed λ_{max} of *SQ1* has been observed at 625 nm is red shifted by 6 nm compared to *SQ2*, so the *SQ1* sensitizer is red shifted than *SQ2* sensitizer.

The ΔG^{inject} of *SQ1* and *SQ2* are 2.5, 3.59 times more than dyenitro and 1.02, 1.12 superior to Cis-SQ dyes. The values of ΔG^{inject} for different hydrazones and azo sensitizers have been previously computed at TD-B3LYP/6-31G* level of theory, e.g. dyenitro (-0.39 and 0.195 eV), 2-{4-[2-p-chlorobenzylidene-hydrazino] phenyl}ethylene-1,1,2-tricarbonitrile (-0.39 and 0.9520), 2-{4-[2-p-chlorobenzylidenehydrazino] phenyl}-ethylene-1,1,2-tricarbonitrile and 2-{4-[2-p-bromobenzylidenehydrazino] phenyl}ethylene-1,1,2-tricarbonitrile (-0.53 and 0.26 eV), respectively [43], and the azo dye 3-(4-methyl-phenylazo)-6-(4-nitro-phenylazo)-2,5,7-triaminopyrazolo [1,5-a] pyrimidine (-1.19 and 0.53 eV) [58] reveal improved electron injection in the set analyzed here. The calculated *f* and ΔG^{inject} values *SQ1* & *SQ2* sensitizers reveal electron injection in these dye would be superior to above mentioned hydrazine, azo dyes and Cis-SQ dyes. The LHE of *SQ1* & *SQ2* sensitizers are greater than the dyenitro, and Cis-SQ dyes see **Table 3**. The greater LHE values of *SQ1* & *SQ2* sensitizers than dyenitro (0.9985 and -0.39), 2-{4-[2-p-chlorobenzylidenehydrazino] phenyl}-ethylene-1,1,2-tricarbonitrile and 2-{4-[2-p-

bromobenzylidenehydrazino] phenyl} ethylene-1, 1,2-tricarbonitrile (0.9848 and 0.53), resp -ectively [43]; the azo dye 3-(4-methyl- phenyl -zo)-6-(4-nitro-phenylazo)-2, 5, 7-triaminopyrazolo [1, 5-a] pyrimidine (0.8732 and -0.86) [78], and Cis-SQ dyes (0.9985 and 0.9807) [50] illuminate that *SQ1* sensitizer would be proficient material for DSSCs.

Open-circuit voltage (V_{oc})

The open-circuit voltage (V_{oc}) is generally measured only experimentally, it means the relationship among the electronic structure of the squaraine dyes and these quantities are unknown till now. The energy relationship can be obtained according to the sensitized mechanism, single electron and single state approximation as under [59]:

$$eV_{oc} = E_{LUMO} - E_{CB} \quad (7)$$

In 2001, Brabec et.al mentions that the V_{oc} depends on the E_{LUMO} [59], and concluded that the larger values of the E_{LUMO} would lead higher V_{oc} . The reduction potential (E_{LUMO}) of the *SQ1* is greater than the *SQ2*, mean that the V_{oc} of *SQ1* sensitizer would be larger than that of *SQ2* counterpart, this is due to the -COOH group is favorable site to transfer the electrons from dyes to TiO_2 surface.

Conclusions

New *SQ1* and *SQ2* indole-based squaraine sensitizers suitable for DSSCs have been synthesized. The theoretical calculations and absorbance results show that the electron density of LUMO of *SQ1* is delocalized in the whole chromophore, leading to strong electronic coupling between *SQ1* and TiO_2 surface. So, the *SQ1* sensitized solar cells exhibit better photovoltaic performance. The *SQ1* showed significant effect towards the red shifts in the absorption spectra due to carboxylic groups. The electron donating group -OCH₃ increases the energies while the -COOH group decreases the energies of HOMOs and LUMOs. The greater and voltage open circuit (V_{oc}) of *SQ1* and *SQ2* indole-based squaraine dyes compared to the corresponding values in the dyenitro (2-{4-[2-p-chlorobenzylidenehydrazino]phenyl}-ethylene-1, 1,2-, 2-{4-[2-p-bromobenzylidenehydrazino]phenyl} ethylene-1,1,2-tricarbonitrile) and Cis-SQ dyes reveal that the *SQ1* and *SQ2* sensitizers would be efficient dye-sensitized solar cells materials. The enhanced electron injection and light harvesting efficiencies of indole-based squaraine dyes would lead improved short-circuit current density (J_{sc}) than the referenced sensitizers which would be proficient DSSCs materials [50, 58]. We hope this work will be helpful to improve the performance of DSSc.

References

- Grätzel, M.; *Nature.*, **2001**, 414, 338-344.
DOI: [10.1038/35104607](https://doi.org/10.1038/35104607)
- Qin, C.; Wong, W-Y.; Han, L.; Regan, O.; Gratzel, B; *M Nat.*, **1991**, 353, 737. **2013**, 8, 1706-1719.
DOI: [10.1002/asia.201300185](https://doi.org/10.1002/asia.201300185)
- Günes, S.; Sariciftci, NS.; *Inorganica Chim Acta.*, **2008**, 361, 581-588.
DOI: [10.1016/j.ica.2007.06.042](https://doi.org/10.1016/j.ica.2007.06.042)
- El-Shishtawy, RM.; *Int. J. Photoenergy.*, **2009**, 2009.
DOI: [10.1155/2009/434897](https://doi.org/10.1155/2009/434897)
- Das, S.; Thomas, KG.; George, M V.; *Mol. Supramol Photochem.*, **1997**, 1, 467-518.
- Stoll, RS.; Severin, N.; Rabe, JP.; Hecht, S.; *Adv. Mater.*, **2006**, 18, 1271-1275.
DOI: [10.1002/adma.200502094](https://doi.org/10.1002/adma.200502094)
- LAW, K-Y.; *J. imaging. Sci.*, **1987**, 31, 172-177.
- Zhang, G.; Bala, H.; Cheng, Y.; et al.; *Chem. Commun.*, **2009**, 16, 2198-2200.
DOI: [10.1039/B822325D](https://doi.org/10.1039/B822325D)
- Lan, Y-K.; Huang, C-L.; *J. Phys. Chem. B.*, **2008**, 47, 14857-14862.
DOI: [10.1021/jp806967x](https://doi.org/10.1021/jp806967x)
- Weitz, RT.; Amsharov, K.; Zschieschang, U.; et al.; *J. Am. Chem. Soc.*, **2008**, 14, 4637-4645.
DOI: [10.1021/ja074675e](https://doi.org/10.1021/ja074675e)
- Newman, CR.; Frisbie, CD.; da Silva Filho, DA.; Brédas, J-L.; Ewbank, PC.; Mann, KR.; *Chem. Mater.*, **2004**, 23, 4436-4451.
DOI: [10.1021/cm049391x](https://doi.org/10.1021/cm049391x)
- Zaumseil, J.; Siringhaus, H.; *Chem. Rev.*, **2007**, 4, 1296-1323.
- Katoh, R.; Furube, A.; Yoshihara, T.; et al.; *J. Phys. Chem. B.*, **2004**, 15, 4818-4822.
DOI: [10.1021/cr0501543](https://doi.org/10.1021/cr0501543)
- Beverina, L.; Salice, P.; *European. J. Org. Chem.*, **2010**, 7, 1207-1225.
DOI: [10.1002/ejoc.200901297](https://doi.org/10.1002/ejoc.200901297)
- Mori, T.; Kim, H-G.; Mizutani, T.; Lee, D-C.; *Jpn. J. Appl. Phys.*, **2001**, 9R, 5346.
- Chen, G.; Sasabe, H.; Sasaki, Y.; et al.; *Chem. Mater.*, **2014**, 3, 1356-1364.
DOI: [10.1021/cm4034929](https://doi.org/10.1021/cm4034929)
- Silvestri, F.; Irwin, MD.; Beverina, L.; Facchetti, A.; Pagani, GA.; Marks, TJ.; *J. Am. Chem. Soc.*, **2008**, 52, 17640-17641.
DOI: [10.1021/ja806787](https://doi.org/10.1021/ja806787)
- Bagnis, D.; Beverina, L.; Huang, H.; et al.; *J. Am. Chem. Soc.*, **2010**, 12, 4074-4075.
DOI: [10.1021/ja100520q](https://doi.org/10.1021/ja100520q)
- Irfan, A.; Cui, R.; Zhang, J.; *Theor. Chem. Acc.*, **2009**, 5-6, 275-281.
DOI: [10.1007/s00214-009-0506-3](https://doi.org/10.1007/s00214-009-0506-3)
- Venkataraman, L.; Klare, JE.; Nuckolls, C.; Hybertsen, MS.; Steigerwald, ML.; *Nature.*, **2006**, 7105, 904-907.
DOI: [10.1038/nature05037](https://doi.org/10.1038/nature05037)
- Fu, Y-T.; da Silva Filho, DA.; Sini, G.; et al.; *Adv Funct Mater.*, **2014**, 24, 3790-3798.
DOI: [10.1002/adfm.201303941](https://doi.org/10.1002/adfm.201303941)
- Yen, Y-S.; Chou, H-H.; Chen, Y-C.; Hsu, C-Y.; Lin, JT.; *J. Mater. Chem.*, **2012**, 18, 8734-8747.
DOI: [10.1039/C2JM30362K](https://doi.org/10.1039/C2JM30362K)
- Ruankham, P.; Macaraig, L.; Sagawa, T.; Nakazumi, H.; Yoshikawa, S.; *J. Phys. Chem. C.*, **2011**, 48, 23809-23816.
DOI: [10.1021/jp204325y](https://doi.org/10.1021/jp204325y)
- Ooyama, Y.; Harima, Y.; *European. J. Org. Chem.*, **2009**, 18, 2903-2934.
DOI: [10.1002/ejoc.200900236](https://doi.org/10.1002/ejoc.200900236)
- Mishra, A.; Fischer, MKR.; Bäuerle, P.; *Angew. Chemie. Int. Ed.*, **2009**, 14, 2474-2499.
DOI: [10.1002/anie.200804709](https://doi.org/10.1002/anie.200804709)
- Al-Sehemi, AG.; Irfan, A.; Asiri, AM.; Ammar, YA.; *Spectrochim. Acta. A. Mol. Biomol. Spectrosc.*; **2012**, 91, 239-243
DOI: [10.1016/j.saa.2012.01.016](https://doi.org/10.1016/j.saa.2012.01.016)
- Al-Sehemi, AG.; Irfan, A.; Asiri, AM.; Ammar, YA.; *J. Mol. Struct.*; **2012**, 1019,130-134.
DOI: [10.1016/j.molstruc.2012.02.035](https://doi.org/10.1016/j.molstruc.2012.02.035)
- Irfan, A.; Hina, N.; Al-Sehemi, A.; Asiri, A.; *J. Mol. Model.*; **2012**, 18, 4199- 4207.
DOI: [10.1007/s00894-012-1421-4](https://doi.org/10.1007/s00894-012-1421-4)
- Al-Sehemi, A.; Irfan, A.; Asiri, A.; *Theor. Chem. Acc.*; **2012**, 131, 1-10.
DOI: [10.1007/s00214-012-1199-6](https://doi.org/10.1007/s00214-012-1199-6)

30. Irfan, A.; Al-Sehemi, A.; *J. Mol. Model.*; **2012**, 18:4893–4900.
DOI: [10.1007/s00894-012-1488-y](https://doi.org/10.1007/s00894-012-1488-y)
31. Irfan, A.; Jin, R.; Al-Sehemi, AG.; Asiri, AM.; *Spectrochim. Acta. A. Mol. Biomol. Spectrosc.*; **2013**, 110, 60–66.
DOI: [10.1016/j.saa.2013.02.045](https://doi.org/10.1016/j.saa.2013.02.045)
32. Preat, J.; Jacquemin, D.; Perpète, EA.; *Environ. Sci. Technol.*; **2010**, 44, 5666–5671.
DOI: [10.1021/es100920j](https://doi.org/10.1021/es100920j)
33. Liu, D.; Fessenden, RW.; Hug, GL.; Kamat, PV.; *J. Phys. Chem. B.*; **1997**, 101, 2583–2590.
DOI: [10.1021/jp962695p](https://doi.org/10.1021/jp962695p)
34. Burfeindt, B.; Hannappel, T.; Storck, W.; Willig, F.; *J. Phys. Chem.*; **1996**, 100, 16463–16465.
DOI: [10.1021/jp9622905](https://doi.org/10.1021/jp9622905)
35. Sayama, K.; Tsukagoshi, S.; Hara, K, et al.; *J. Phys. Chem. B.*; **2002**, 106, 1363–1371.
DOI: [10.1021/jp0129380](https://doi.org/10.1021/jp0129380)
36. AL-Fahdan, NS.; Asiri, A.; Irfan, A.; Basaif, SA.; El-Shishtawy, R M.; *J. Mol. Model.*; **2014**, 20:2517
DOI: [10.1007/s00894-014-2517-9](https://doi.org/10.1007/s00894-014-2517-9)
37. Alex, S.; Santhosh, U.; Das, S.; *J. Photochem. Photobiol. A Chem.*, **2005**, 1, 63–71.
DOI: [10.1016/j.jphotochem.2004.11.005](https://doi.org/10.1016/j.jphotochem.2004.11.005)
38. Fabian, J.; Nakazumi, H.; Matsuoka, M.; *Chem. Rev.*, **1992**, 6, 1197–1226.
DOI: [10.1021/cr00014a003](https://doi.org/10.1021/cr00014a003)
39. Basheer, MC.; Alex, S.; Thomas, KG.; Suresh, CH.; Das, S.; *Tetrahedron.*, **2006**, 4, 605–610.
DOI: [10.1016/j.tet.2005.10.012](https://doi.org/10.1016/j.tet.2005.10.012)
40. Sreejith, S.; Carol, P.; Chithra, P.; Ajayaghosh, A.; *J. Mater. Chem.*, **2008**, 3, 264–274.
DOI: [10.1039/B707734C](https://doi.org/10.1039/B707734C)
41. 38. Kong, F.; Dai, S.; Wang, K.; *Adv. Optoelectron.*, **2007**, 2007, 1–14.
DOI: [10.1155/2007/75384](https://doi.org/10.1155/2007/75384)
42. Guillaumont, D.; Nakamura, S.; *Dye. Pigment.*, **2000**, 2, 85–92.
DOI: [10.1016/S0143-7208\(00\)00030-9](https://doi.org/10.1016/S0143-7208(00)00030-9)
44. Irfan, A.; Hina, N.; Al-Sehemi, AG.; Asiri, AM.; *J. Mol. Model.*, **2012**, 9, 4199–4207.
DOI: [10.1007/s00894-012-1421-4](https://doi.org/10.1007/s00894-012-1421-4)
45. Irfan, A.; Al-Sehemi, AG.; Al-Assiri, MS.; *J. Mol. Graph. Model.*, **2013**, 44, 168–176.
DOI: [10.1016/j.jmgm.2013.06.003](https://doi.org/10.1016/j.jmgm.2013.06.003)
46. Irfan, A.; Al-Sehemi, AG.; Kalam, A.; *J. Mol. Struct.*, **2013**, 1049, 198–204.
DOI: [10.1016/j.molstruc.2013.06.023](https://doi.org/10.1016/j.molstruc.2013.06.023)
47. Irfan, A.; Al-Sehemi, AG.; Muhammad, S.; *Synth. Met.*, **2014**, 190, 27–33.
DOI: [10.1016/j.synthmet.2014.01.017](https://doi.org/10.1016/j.synthmet.2014.01.017)
48. Sánchez-Carrera, RS.; Coropceanu, V.; da Silva Filho, DA.; et al.; *J. Phys. Chem. B.*, **2006**, 38, 18904–18911.
DOI: [10.1021/jp057462p](https://doi.org/10.1021/jp057462p)
49. Wong, BM.; Cordaro, JG.; *J. Chem. Phys.*, **2008**, 21, 214703.
DOI: [10.1063/1.3025924](https://doi.org/10.1063/1.3025924)
50. Zhang, C.; Liang, W.; Chen, H.; Chen, Y.; Wei, Z.; Wu, Y.; *J. Mol. Struct. THEOCHEM.*, **2008**, 1, 98–104.
DOI: [10.1016/j.theochem.2008.04.035](https://doi.org/10.1016/j.theochem.2008.04.035)
51. Huong, VTT.; Nguyen, HT.; Tai, TB.; Nguyen, MT.; *J. Phys. Chem. C.*, **2013**, 19, 10175–10184.
DOI: [10.1021/jp401191a](https://doi.org/10.1021/jp401191a)
52. Asbury, JB.; Wang, Y-Q.; Hao, E.; Ghosh, HN.; Lian, T.; *Res. Chem. Intermed.*, **2001**, 4, 393–406.
DOI: [10.1163/156856701104202255](https://doi.org/10.1163/156856701104202255)
53. Hagfeldt, A.; Graetzel, M.; *Chem. Rev.*, **1995**, 1, 49–68.
DOI: [10.1021/cr00033a003](https://doi.org/10.1021/cr00033a003)
54. AL-Fahdan, NS.; Asiri, AM.; Irfan, A.; Basaif, SA.; El-Shishtawy, RM.; *J. Mol. Model.*, **2014**, 12, 1–9.
DOI: [10.1007/s00894-014-2517-9](https://doi.org/10.1007/s00894-014-2517-9)
55. Irfan, A.; Cui, R.; Zhang, J.; Hao, L.; *Chem. Phys.*; **2009**, 364, 39–45.
DOI: [10.1016/j.chemphys.2009.08.009](https://doi.org/10.1016/j.chemphys.2009.08.009)
56. Robertson, N.; *Angew. Chem. Int. Ed.*; **2006**, 45, 2338–2345.
DOI: [10.1002/anie.200503083](https://doi.org/10.1002/anie.200503083)
57. Brabec, CJ.; Cravino, A.; Meissner, D.; et al.; *Adv. Funct. Mater.*, **2001**, 5, 374–380.
58. Irfan, A.; *Mater. Chem. Phys.*; **2013**, 142, 238–247.
DOI: [10.1016/j.matchemphys.2013.07.011](https://doi.org/10.1016/j.matchemphys.2013.07.011)
59. Zhou, Y.; Eck, M.; Veit, C.; et al.; *Sol. Energy. Mater. Sol. Cells.*; **2011**, 95, 1232–1237.
DOI: [10.1016/j.solmat.2010.12.041](https://doi.org/10.1016/j.solmat.2010.12.041)
60. Celik, D.; Krueger, M.; Veit, C.; et al.; *Sol. Energy. Mater. Sol. Cells.*; **2012**, 98, 433–440.
DOI: [10.1016/j.solmat.2011.11.049](https://doi.org/10.1016/j.solmat.2011.11.049)
61. Al-Sehemi, AG.; Irfan, A.; Al-Melfi, MAM.; Al-Ghamdi, AA.; Shalaan, E.; *J. Photochem. Photobiol. A. Chem.*; **2014**, 292, 1–9.
DOI: [10.1016/j.jphotochem.2014.07.003](https://doi.org/10.1016/j.jphotochem.2014.07.003)
62. Al-Sehemi, AG.; Irfan, A.; Fouda, AM.; *Spectrochim. Acta. A. Mol. Biomol. Spectrosc.*; **2013**, 111, 223–229.
DOI: [10.1016/j.saa.2013.04.010](https://doi.org/10.1016/j.saa.2013.04.010)
63. Pourtois, G.; Beljonne, D.; Cornil, J.; Ratner, MA.; Brédas, JL.; *J. Am. Chem. Soc.*, **2002**, 16, 4436–4447.
DOI: [10.1021/ja017150+](https://doi.org/10.1021/ja017150+)
64. Asiri, AM.; Al-Horaibi, SAH.; Irfan, A.; Basaif, SA.; El-Shishtawy, RM.; *Int. J. Electrochem. Sci.*; **2015**, 10, 1529 - 1542.